REVIEW

Open Access

CrossMark

Asteroid spin-rate studies using large sky-field surveys

Chan-Kao Chang[1*] ○, Hsing-Wen Lin[1], Wing-Huen Ip[1,2], Thomas A. Prince[3], Shrinivas R. Kulkarni[3], David Levitan[3], Russ Laher[4] and Jason Surace[4]

Abstract

Eight campaigns to survey asteroid rotation periods have been carried out using the intermediate Palomar Transient Factory in the past 3 years. 2780 reliable rotation periods were obtained, from which we identified two new super-fast rotators (SFRs), (335433) 2005 UW163 and (40511) 1999 RE88, and 23 candidate SFRs. Along with other three known super-fast rotators, there are five known SFRs so far. Contrary to the case of rubble-pile asteroids (i.e., bounded aggregations by gravity only), an internal cohesion, ranging from 100 to 1000 Pa, is required to prevent these five SFRs from flying apart because of their super-fast rotations. This cohesion range is comparable with that of lunar regolith. However, some candidates of several kilometers in size require unusually high cohesion (i.e., a few thousands of Pa). Therefore, the confirmation of these kilometer-sized candidates can provide important information about asteroid interior structure. From the rotation periods we collected, we also found that the spin-rate limit of C-type asteroids, which has a lower bulk density, is lower than for S-type asteroids. This result is in agreement with the general picture of rubble-pile asteroids (i.e., lower bulk density, lower spin-rate limit). Moreover, the spin-rate distributions of asteroids of $3 < D < 15$ km in size show a steady decrease along frequency for $f > 5$ rev/day, regardless of the location in the main belt. The YORP effect is indicated to be less efficient in altering asteroid spin rates from our results when compared with the flat distribution found by Pravec et al. (Icarus 197:497–504, 2008. doi:10.1016/j.icarus.2008.05.012). We also found a significant number drop at $f = 5$ rev/day in the spin-rate distributions of asteroids of $D < 3$ km.

Keywords: Minor planets, Asteroids: general – surveys

Introduction

From the asteroid spin-rate distribution, we can understand the mechanisms altering asteroid spin status. In addition, the asteroid spin-rate limit also provides a practical way to investigate the asteroid interior structure. However, a comprehensive understanding of the aforementioned questions depends on a large sample of asteroid spin rates. Thanks to advanced technology—wide-field detectors, high computing power, massive data storage, and robotic observation—it is possible to obtain numerous asteroid light curves within a short period of time to derive hundreds of asteroid rotation periods.

It is believed that asteroids with diameter of $D > 0.15$ km have "rubble-pile" structure, in which asteroids are gravitationally bounded aggregations with no assumed internal cohesion. Therefore, a rubble-pile asteroid cannot rotate exceedingly fast, otherwise the centrifugal force would overcome the gravity, which consequently would lead to the breakup of the asteroid. This idea is supported by the "2.2-h spin barrier"[1] held for asteroids of $D > 0.15$ km (Harris 1996; Pravec and Harris 2000). On the other hand, the asteroids of $D < 0.15$ km can rotate faster than the 2.2-h spin barrier because of their monolithic structure. However, 2001 OE84, an asteroid of $D \sim 0.65$ km that completes 1 rotation in 29.19 min, demonstrates the first exception among the rubble-pile asteroids (Pravec et al. 2002), and it is,

*Correspondence: rex@astro.ncu.edu.tw
[1] Institute of Astronomy, National Central University, No. 300, Zhongda Rd., Zhongli Dist., 32001 Taoyuan, Taiwan
Full list of author information is available at the end of the article

---

[1] The 2.2-h spin barrier was calculated assuming a bulk density 3 g cm^{-3} for asteroids.

Chang *et al. Geosci. Lett.* (2017) 4:17

Page 2 of 8

therefore, called a "super-fast rotator" (SFR). To explain the presence of 2001 OE84, Holsapple et al. (2007) introduced the concept of internal cohesive strength into the rubble-pile structure. This idea allows a transition zone between monolithic and rubble-pile asteroids to accommodate SFRs. If this model is realistic, a certain number of SFRs should be found among the rubble-pile asteroids. Therefore, the physical properties of SFRs provide important information for understanding asteroid interior structure. Moreover, another important implication of rubble-pile structure is that the lower the bulk density of an asteroid, the longer its spin barrier can be expected.[2] With enough samples of rotation period and taxonomy type, we should be able to see different spin-rate limits for different types of asteroids.

In addition, we can study how the spin status of asteroids can be affected by mutual collisions and the Yarkovsky–O'Keefe–Radzievskii–Paddack (YORP) effect from the spin-rate distribution of asteroid. When an asteroid system stays in a collisional equilibrium state, it should have a Maxwellian spin-rate distribution (Salo 1987), which has been observed indeed for asteroids of $D > 40$ km (Pravec et al. 2002). To the contrary, a number excess was found both in the slow and fast ends of the spin-rate distribution for asteroids of $3 < D < 15$ km (i.e., a flat form, the number in each spin-rate bin is similar) (Pravec et al. 2008), which indicates a non-collisional equilibrium system. It is believed that the YORP effect, which can alter the spin rates of asteroids of few kilometers in size within a million-year timescale (Rubincam 2000), creates the aforementioned excesses in the both ends of the distribution (Pravec et al. 2008). However, more recent results from large sky surveys show a different spin-rate distribution of asteroids of $3 < D < 15$ km, which is more like a Maxwellian form (Masiero et al. 2009; Polishook et al. 2012). These two forms of distributions of asteroids of $3 < D < 15$ km suggest different scenarios of spin-status evolution. Although the YORP effect accounts for both distributions (e.g., flat distribution vs. Maxwellian-like distribution), a different degree of spin-status alteration would be required for each case.

Along this story line, we initiated our asteroid spin-rate study using the iPTF[3] to collect numerous asteroid light curves with wide sky coverage since February 2013. As a report presented at the AOGS 2016 conference, this article summarizes our work conducted over the past 3 years. We organize this article in the following way: a brief introduction of the data survey and rotation-period

analysis is given in "Data survey and rotation-period analysis" section; the results and discussion are presented in "Results and discussion" section; and the summary and conclusions can be found in "Summary" section.

Data survey and rotation-period analysis

Data survey

The iPTF is a project to explore the transient and variable sky synoptically. Utilizing the Palomar 48-inch Oschin Schmidt Telescope and an 11-chip mosaic CCD camera, the iPTF has a field of view of $\sim$7.26 deg^2 (Law et al. 2009; Rau et al. 2009). Most of the iPTF exposures were taken in the Mould-R band, and the other available filters include the Gunn-g' and four different H_α bands. The exposure time of the iPTF is fixed to 60 s, which can routinely reach a limiting magnitude of $R \sim 21$ mag at the 5σ level (Law et al. 2010).
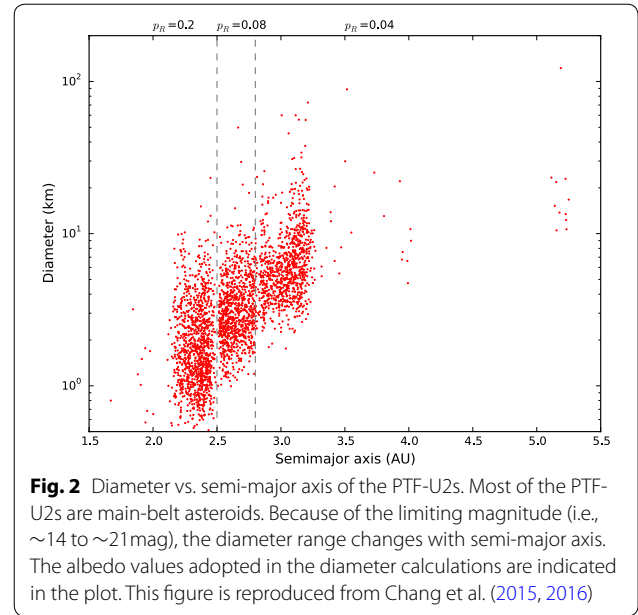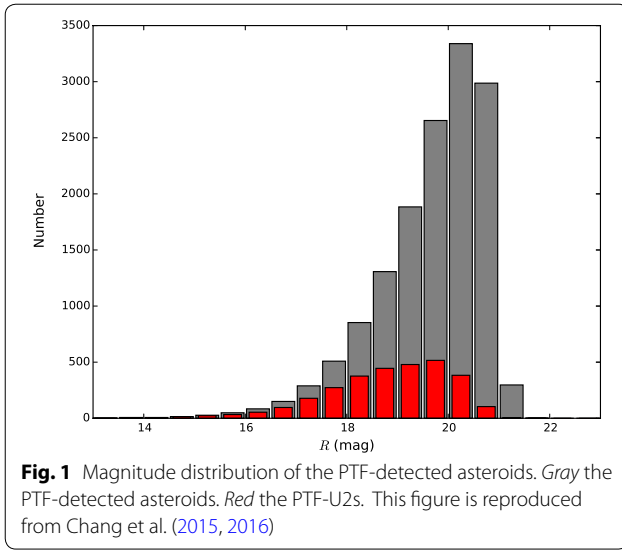
All iPTF exposures are processed by the IPAC-PTF photometric pipeline (Grillmair et al. 2010; Laher et al. 2014). The absolute magnitude is calibrated against Sloan Digital Sky Survey fields (SDSS) (York et al. 2000), and the accuracy can reach $\sim$0.02 mag for the so-called photometric nights (Ofek et al. 2012a, b).

In order to collect a large number of asteroid light curves, we initiated a survey for asteroid spin rates using the iPTF since February 2013. Until early in 2015, we carried out eight campaigns, including (1) three sets of observations of 12 fields at 20-min cadence in four adjacent nights, in 15–18 February 2013, 6–9 January 2014 , and 20–23 February 2014 (Chang et al. 2014a, b, 2015); and (2) four sets of observations of 6 fields at 10-min cadence in two/three adjacent nights, in 29–31 October 2014, 10–13 November 2014 , 18–19 January 2015 , 20–21 February 2015, and 25–26 February 2015 (Chang et al. 2016). The total sky coverage was $\sim$450 deg^2. More details about each campaign are available in the original published papers, please see (Chang et al. 2014a, b, 2015, 2016).

To extract the light curves of known asteroids, we first removed all stationary sources from the iPTF catalogs, and then matched all residual detections against the ephemerides obtained from the *JPL/HORIZONS* system within a search radius of two arc seconds. We also excluded all detections flagged as defective by the IPAC-PTF photometric pipeline from the extracted light curves. We finally obtained $\sim$17,000 asteroid light curves, each with number of detections $\geq$10 (hereafter, PTF-detected asteroids), which were then subjected to period analysis (see below for details). The magnitude distribution of the PTF-detected asteroids is given in Fig. 1, which ranges from $\sim$14 to $\sim$21 mag; a comparable histogram is also shown for the smaller subset of asteroids that we determined to have reliable rotation

---

[2] $P \sim 3.3\sqrt{(1 + \Delta m)/\rho}$, where P is rotation period in hour, Δm is lightcurve variation in magnitude, and ρ is bulk density in g cm^{-3} (Harris 1996; Pravec and Harris 2000).

[3] Intermediate Palomar Transient Factory; http://ptf.caltech.edu/iptf.

Chang *et al. Geosci. Lett.* (2017) 4:17

Page 3 of 8

Fig. 1 Magnitude distribution of the PTF-detected asteroids. *Gray* the PTF-detected asteroids. *Red* the PTF-U2s. This figure is reproduced from Chang et al. (2015, 2016)

Fig. 2 Diameter vs. semi-major axis of the PTF-U2s. Most of the PTF-U2s are main-belt asteroids. Because of the limiting magnitude (i.e., ∼14 to ∼21mag), the diameter range changes with semi-major axis. The albedo values adopted in the diameter calculations are indicated in the plot. This figure is reproduced from Chang et al. (2015, 2016)

periods (hereafter, PTF-U2s; see next subsection for more details).

We adopted the diameter estimations of the *WISE/NEOWISE* measurements (Grav et al. 2011; Mainzer et al. 2011; Masiero et al. 2011), if available, for PTF-detected asteroids. Otherwise, the diameters were estimated using

$$D = \frac{1130}{\sqrt{p_R}} 10^{-H_R/5}, \tag{1}$$

where D is the diameter in km, H_R is the R band absolute magnitude, p_R is the R band geometric albedo, and the conversion constant of 1130 is from Jewitt et al. (2013). We assumed three empirical albedo values in the estimation, which are $p_R = 0.20$, 0.08, and 0.04 for asteroids in the inner ($2.1 < a < 2.5$ AU), mid ($2.5 < a < 2.8$ AU), and outer ($a > 2.8$ AU) main belts, respectively (Tedesco et al. 2005).[4] Figure 2 shows a plot of semi-major axes vs. diameters for the PTF-U2s, where we see that the asteroid diameter range changes along with the semi-major axis due to our limiting magnitude. Therefore, we have only a few asteroids of $D > 15$ km in the inner main belt. The same situation also occurs for the asteroids of $D < 3$ km in the outer main belt.

Rotation-period analysis
To measure the asteroid rotation periods, all light-curve measurements were corrected for light-travel time and placed at both heliocentric, r, and geocentric, $\triangle$, 1 AU distances to obtain reduced magnitudes. The phase

---

[4] A wider range of albedo values for small asteroids has been reported (Usui et al. 2013). However, the albedo value is not available for each object in our sample. Therefore, the empirical albedo values for asteroids at different locations are assumed here.

angles underwent only a small change during our short observation time span for each survey (i.e., ≤4 days). Therefore, we estimate the absolute magnitude simply by applying a fixed G_R slope of 0.15 in the $H–G$ system (Bowell et al. 1989). Then, the traditional second-order Fourier series method was used to derive rotation periods (Harris et al. 1989):

$$
M_{i,j} = \sum_{k=1,2} \left\{ B_k \sin \left[\frac{2\pi k}{P} (t_j - t_0) \right] \right. \\
\left. + C_k \cos \left[\frac{2\pi k}{P} (t_j - t_0) \right] \right\} + Z_i, \tag{2}
$$

where $M_{i,j}$ are the R band reduced magnitudes measured at the light-travel-time-corrected epoch, t_j; B_k and C_k are the Fourier coefficients; P is the rotation period; t_0 is an arbitrary epoch; and the constant values, Z_i, are the zero-point offsets between measurements obtained from different fields, nights, and chips. Since the equation has at least seven to nine parameters to be fitted, we therefore confine our period analysis to the light curves with ≥10 detections. All the derived rotation periods were reviewed by careful eye inspection to determine their reliability according to their folded light curves. We follow the definition in Warner et al. (2009) and assigned a quality code to each derived rotation period, where '3' means highly reliable; '2' means some ambiguity; '1' means possible, but may be wrong. Moreover, when we were unable to find any acceptable solution for a light curve, it was assigned $U = 0$. We finally harvested 2780 reliable rotation periods (i.e., $U \geq 2$; hence, the reason we name them PTF-U2s) from our pool of ∼17,000 PTF-detected asteroids.

Chang *et al. Geosci. Lett.* (2017) 4:17

Page 4 of 8

Results and discussion

Spin-rate limit and super-fast rotators

From our surveys, we identified two new SFRs. Our first SFR is (335433) 2005 UW163, which is a V-type asteroid with a diameter of ∼0.6 km that completes one rotation in 1.29 h (Chang et al. 2014, 2015). Its super-fast rotation was initially identified in the 2014 February survey using the iPTF and then confirmed by 2014 March follow-up observations using the 200-inch Hale Telescope at the Palomar Observatory. The identification of 2005 UW163 as the second SFR after 2001 OE84 ensures the existence of SFR group. Our second SFR is (40511) 1999 RE88, which is a S-type asteroid with a diameter of ∼2 km that completes one rotation period in 1.96 h (Chang et al. 2016). In addition, we also found 23 SFR candidates. Figure 3 shows a plot of rotation periods vs. diameters for the PTF-U2s on top of the data points of $U \geq 2$ obtained from the Asteroid Light Curve Database (LCDB)[5] (Warner et al. 2009).

In general, we see that the majority of rubble-pile asteroids (i.e., $D > 0.15$ km) are all below the 2.2-h spin barrier. Some monolithic objects (i.e., $D < 0.15$ km), however, can have rotation periods shorter than 2.2 h. In addition, the five SFRs, including 2001 OE84 (Pravec et al. 2002), 2000 GD65 (Polishook et al. 2016), and 1950 DA (Rozitis et al. 2014), and the 23 candidates stand out from the rubble-pile asteroids to form a group above the 2.2-h spin barrier that cannot be explained by the rubble-pile structure unless they have anomalously high bulk densities (see Fig. 4). To keep these five SFRs from breaking up, it requires an internal cohesion ranging from several tens to several hundreds of Pa (Chang et al. 2016). This value is similar to that of lunar regolith (i.e., 100 to 1000 Pa) (Mitchell et al. 1974). However, the cohesion for those candidates with relatively large diameters is up to several thousands of Pa, which is almost an order of magnitude larger than that of the five SFRs. Therefore, to elucidate the candidates with relatively large diameters is important to understand asteroid interior structure. When compared with the average asteroids, SFRs are very rare. If internal cohesion can be universally applied to asteroids, we should be able to identify more SFRs. This probably suggests that the SFRs is a peculiar group apart from the typical asteroids.

Spin rate vs. spectral type

In order to know whether the asteroids of different spectral types have various spin-rate limits, we select the asteroids from our PTF-U2s and the LCDB based on both rotation period and SDSS spectral type. We finally have
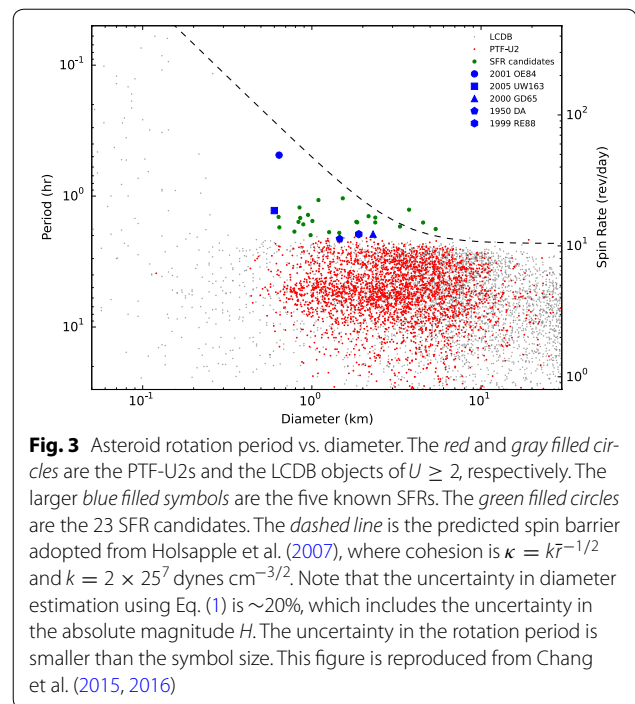

Fig. 3 Asteroid rotation period vs. diameter. The *red* and *gray filled circles* are the PTF-U2s and the LCDB objects of $U \geq 2$, respectively. The larger *blue filled symbols* are the five known SFRs. The *green filled circles* are the 23 SFR candidates. The *dashed line* is the predicted spin barrier adopted from Holsapple et al. (2007), where cohesion is $\kappa = k\bar{r}^{-1/2}$ and $k = 2 \times 25^7$ dynes cm$^{-3/2}$. Note that the uncertainty in diameter estimation using Eq. (1) is ∼20%, which includes the uncertainty in the absolute magnitude *H*. The uncertainty in the rotation period is smaller than the symbol size. This figure is reproduced from Chang et al. (2015, 2016)
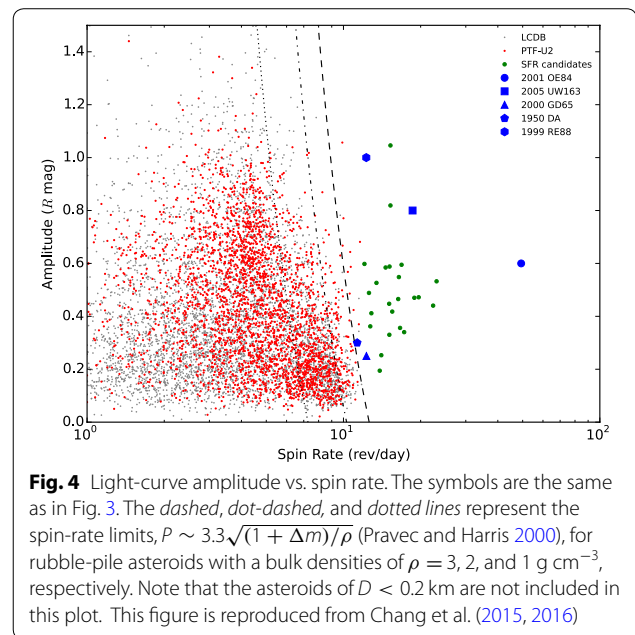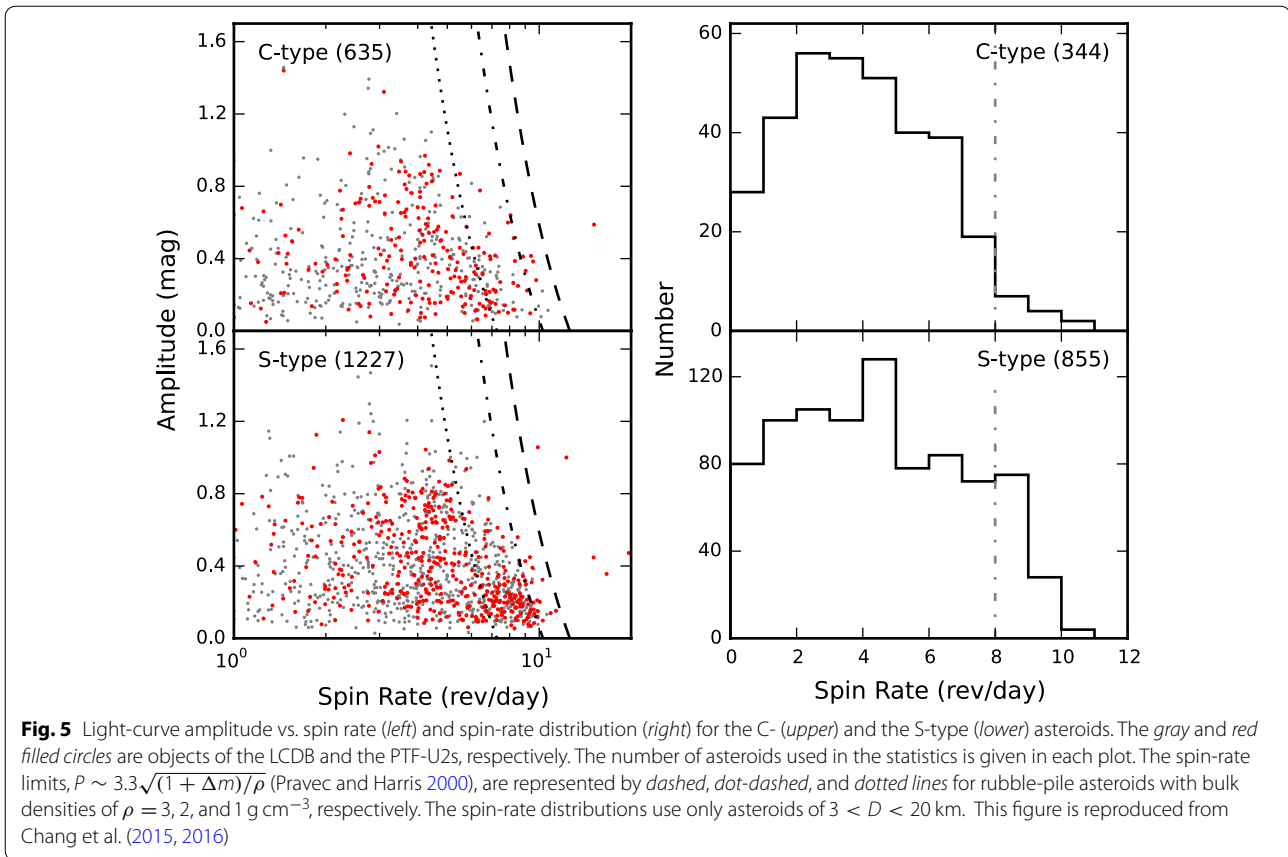

Fig. 4 Light-curve amplitude vs. spin rate. The symbols are the same as in Fig. 3. The *dashed*, *dot-dashed,* and *dotted lines* represent the spin-rate limits, $P \sim 3.3\sqrt{(1 + \Delta m)/\rho}$ (Pravec and Harris 2000), for rubble-pile asteroids with a bulk densities of $\rho = 3, 2$, and 1 g cm^{-3}, respectively. Note that the asteroids of $D < 0.2$ km are not included in this plot. This figure is reproduced from Chang et al. (2015, 2016)

635 C-type asteroids and 1227 S-type asteroids.[6] The left column in Fig. 5 shows plots of light-curve amplitudes vs. spin rates for the C- and S-type asteroids (upper and lower panels, respectively). The C-type asteroids appear to have a boundary around the spin-rate limit for $\rho = 1.5$ g cm^{-3}

---

[5] http://www.minorplanet.info/lightcurvedatabase.html.

[6] Note that not all PTF-U2s have SDDS colors.

Chang *et al. Geosci. Lett. (2017) 4:17*

Page 5 of 8

Fig. 5 Light-curve amplitude vs. spin rate (*left*) and spin-rate distribution (*right*) for the C- (*upper*) and the S-type (*lower*) asteroids. The *gray* and *red filled circles* are objects of the LCDB and the PTF-U2s, respectively. The number of asteroids used in the statistics is given in each plot. The spin-rate limits, $P \sim 3.3\sqrt{(1 + \Delta m)/\rho}$ (Pravec and Harris 2000), are represented by *dashed*, *dot-dashed*, and *dotted lines* for rubble-pile asteroids with bulk densities of $\rho = 3$, 2, and 1 g cm^{-3}, respectively. The spin-rate distributions use only asteroids of $3 < D < 20$ km. This figure is reproduced from Chang et al. (2015, 2016)
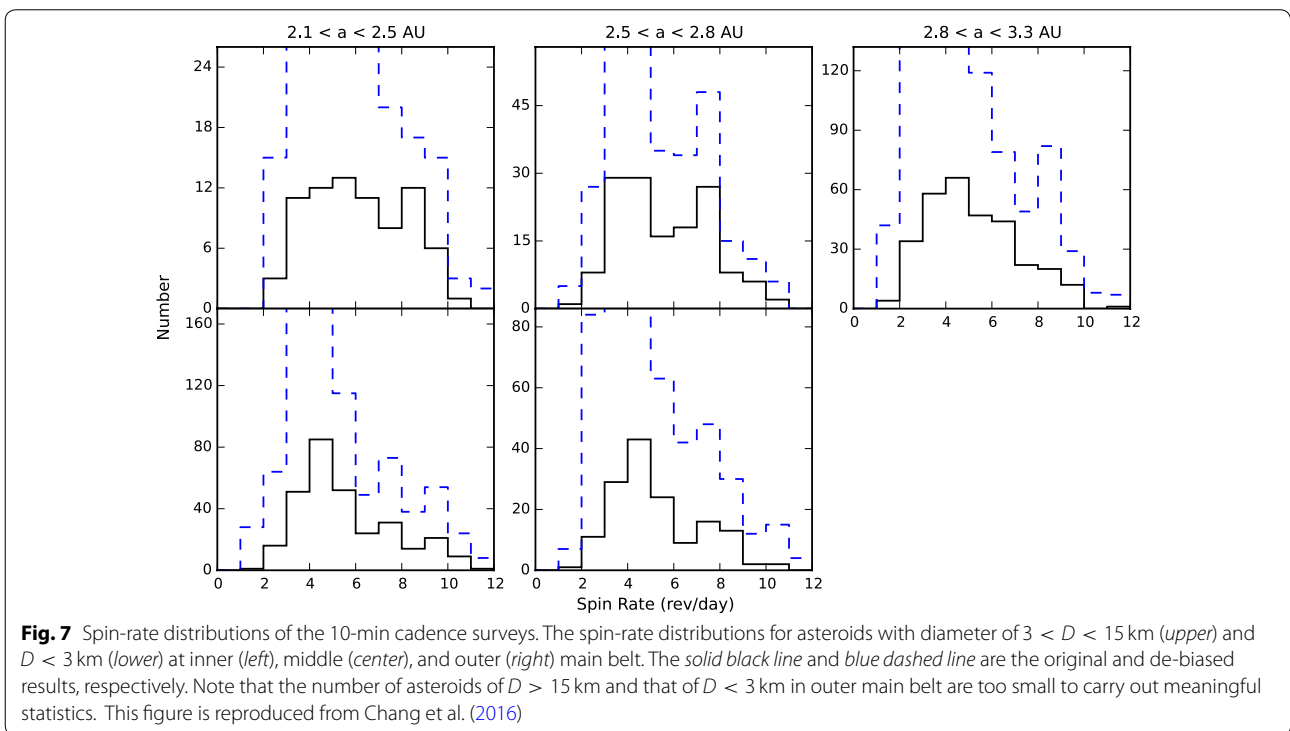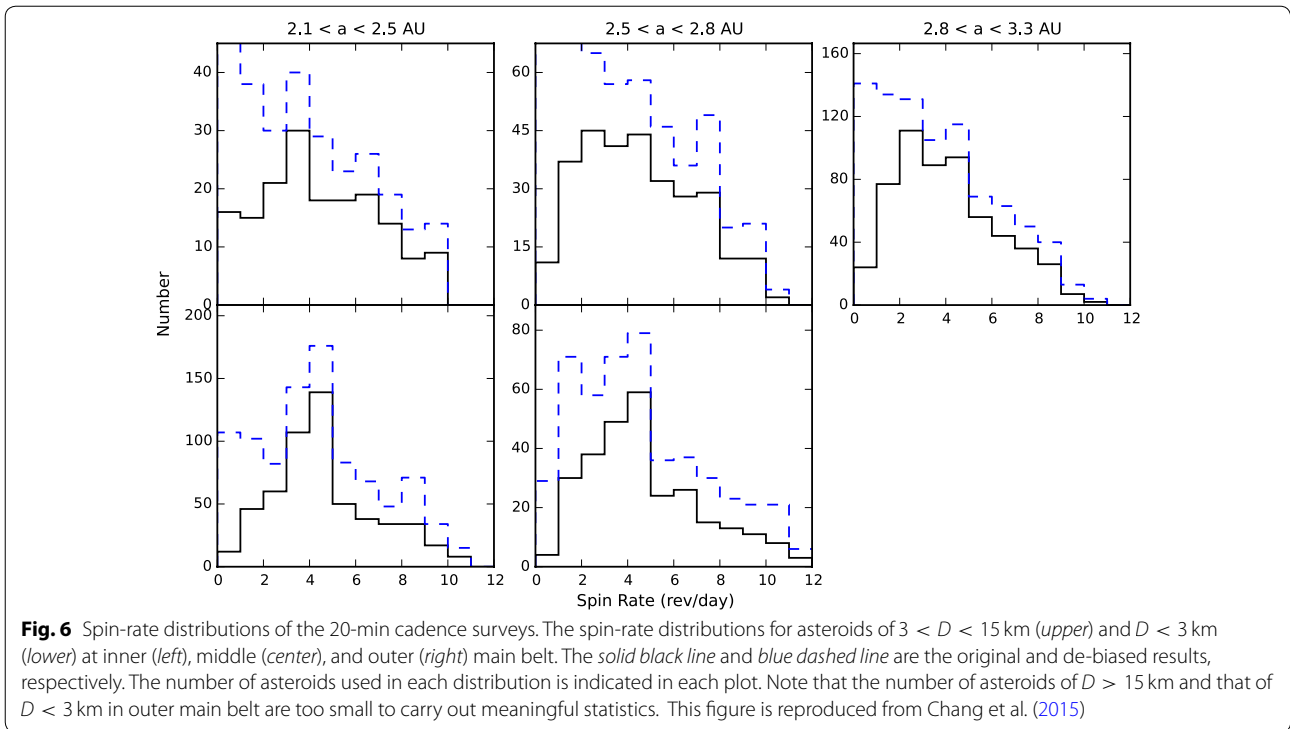
and only a few C-type asteroids can reach the spin-rate limit for $\rho = 2$ g cm^{-3}. On contrary, the S-type asteroids show a clear boundary close to the spin-rate limit for $\rho = 2$ g cm^{-3}. While the C-type has only 22 asteroids (i.e., ∼3%) over the spin-rate limit for $\rho = 1.5$ g cm^{-3}, the S-type has 147 (i.e., ∼12%) asteroids over that limit. This difference becomes more clear in the spin-rate distributions of the C- and S-type asteroids with $3 < D < 20$ km, which is shown in the right panel of Fig. 5. We see that the C-type asteroids have much fewer objects than the S-type for $f > 8$ rev/day. Our results show that the C-type asteroids have a lower spin-rate limit than the S-type asteroids. This is in good agreement with the general picture of rubble-pile structure, in which asteroids with a lower bulk density have a lower spin-rate limit. A similar result was also obtained using the asteroid rotation periods derived from the iPTF archive data (Waszczak et al. 2015). We also suspect that those C-type asteroids with higher spin rates (i.e., $f > 8$ rev/day) could be of the M- or E-type asteroids, which cannot be separated from C-type asteroids using the SDSS color. The M- or E-type asteroids have a higher bulk density, and, therefore, they have a higher spin-rate limit.

The spin-rate distributions

Using the asteroid rotation periods acquired from the iPTF surveys, we are now able to generate the spin-rate distribution as a function of size and location in the main belt. We also take into account the observational bias in our surveys, in which synthetic light curves are used to determine our ability to derive rotation periods according to the survey conditions (see Chang et al. 2015 and the references therein). Figures 6 and 7 show the spin-rate distributions from the 20- and 10-min cadence surveys, respectively. The distributions are separated out for asteroids with $3 < D < 15$ km and $D < 3$ km at the inner ($2.1 < a < 2.5$ AU), middle ($2.5 < a < 2.8$ AU), and outer ($a > 2.8$ AU) main belt. Since the time span of each campaign was only a few days (i.e., 2–4 days depending on the campaign), we were unable to recover relatively long rotation periods (i.e., spin rate $f \leq 3$ rev/day). Therefore, the numbers in the distribution bins for $f \leq 3$ rev/day are greatly biased.

For asteroids with $3 < D < 15$ km, we see that the spin-rate distribution decreases steadily with frequency for $f > 5$ rev/day regardless of their locations in the

Chang *et al. Geosci. Lett.* (2017) 4:17

Page 6 of 8

Fig. 6 Spin-rate distributions of the 20-min cadence surveys. The spin-rate distributions for asteroids of $3 < D < 15$ km (*upper*) and $D < 3$ km (*lower*) at inner (*left*), middle (*center*), and outer (*right*) main belt. The *solid black line* and *blue dashed line* are the original and de-biased results, respectively. The number of asteroids used in each distribution is indicated in each plot. Note that the number of asteroids of $D > 15$ km and that of $D < 3$ km in outer main belt are too small to carry out meaningful statistics. This figure is reproduced from Chang et al. (2015)

Fig. 7 Spin-rate distributions of the 10-min cadence surveys. The spin-rate distributions for asteroids with diameter of $3 < D < 15$ km (*upper*) and $D < 3$ km (*lower*) at inner (*left*), middle (*center*), and outer (*right*) main belt. The *solid black line* and *blue dashed line* are the original and de-biased results, respectively. Note that the number of asteroids of $D > 15$ km and that of $D < 3$ km in outer main belt are too small to carry out meaningful statistics. This figure is reproduced from Chang et al. (2016)

Chang *et al. Geosci. Lett.* (2017) 4:17

Page 7 of 8

main belt. Our result is different from the flat distribution shown by Pravec et al. (2008). This suggests that the timescale of the YORP effect to alter asteroid spin rates is probably longer than expected.

For asteroids with $D < 3$ km, we note an abrupt number drop from $f = 5$ rev/day to $f = 6$ rev/day in the spin-rate distributions. We also find fewer large-amplitude objects (i.e., $\Delta m > 0.2$ mag) in the bins of $f > 6$ rev/day. Because the timescale of the YORP effect is smaller for asteroids of $D < 3$ km, and, moreover, the spin-rate limit is lower for asteroids with large amplitude, we believe that these large-amplitude small asteroids might have been spun up to reach their lower spin-rate limit and, as a consequence, have been broken up into smaller, harder-to-detect pieces. This explains the aforementioned steep number drop, as well.

Summary

To look for SFRs and to conduct a comprehensive study on asteroid rotation, we initiated a project to survey asteroid rotation periods using the iPTF since February 2013. To date, eight campaigns have been carried out, and valuable data have been acquired.

From our survey, we identified two SFRs, (335433) 2005 UW163 and (40511) 1999 RE88, and 23 candidates. (335433) 2005 UW163 is the second SFR to be discovered, which ensures the existence of the SFR group. However, the population size of SFRs is very small compared to that of average asteroids.

The internal cohesion of those candidates with relatively large diameters (i.e., $D > 3$ km) is up to thousands of Pa. This value is an order of magnitude larger than that for the five known SFRs. Future confirmation of their super-fast rotations will provide important information about asteroid interior structure.

With the collected asteroid rotation periods, we found a lower spin-rate limit for C-type asteroids (i.e., lower bulk density) when compared with S-type asteroids. This follows the general concept of rubble-pile asteroids in that the lower their bulk density, the lower their spin-rate limit.

We generated spin-rate distributions for asteroids according to their size and locations in the main belt. The spin-rate distributions of asteroids of $3 < D < 15$ km decrease steadily with frequency for $f > 5$ rev/day, regardless of their locations in the main belt. This might suggest that the timescale of the YORP effect to alter asteroid spin rate is longer than expected. We also find a significant number drop from $f = 5$ to $f = 6$ rev/day in the spin-rate distributions for asteroids of $D < 3$ km. Moreover, the results show a shortfall in the number of large-amplitude, small-size asteroids for $f > 6$ rev/day. The possible explanation is that the large-amplitude, small-size asteroids have been spun up to reach their lower spin-rate limit, and, consequently, this led to them breaking apart.

Authors' contributions
CKC designed and carried out the study, and wrote the paper. HWL and WHI provided valuable suggestions, comments, and help to the study. TAP, SRK, DL, RL, and JS are the key contributors to the iPTF project. All authors read and approved the final manuscript.

Author details
[1] Institute of Astronomy, National Central University, No. 300, Zhongda Rd., Zhongli Dist., 32001 Taoyuan, Taiwan. [2] Space Science Institute, Macau University of Science and Technology, Administration Building, Block A, Avenida Wai Long, Taipa, Macau. [3] Division of Physics, Mathematics and Astronomy, California Institute of Technology, MC 249-17, 1200 East California Blvd, Pasadena, CA 91125, USA. [4] Spitzer Science Center, California Institute of Technology, M/S 314-6, 1200 East California Blvd, Pasadena, CA 91125, USA.

Publisher's Note
Springer Nature remains neutral with regard to jurisdictional claims in published maps and institutional affiliations.

References
Bowell E, Hapke B, Domingue D, Lumme K, Peltoniemi J, Harris AW (1989) Application of photometric models to asteroids. In: Binzel RP, Gehrels T, Matthews MS (eds) Asteroids II. pp 524–556

Chang C-K, Ip W-H, Lin H-W, Cheng Y-C, Ngeow C-C, Yang T-C, Waszczak A, Kulkarni SR, Levitan D, Sesar B, Laher R, Surace J, Prince TA (2014a) 313 new asteroid rotation periods from Palomar Transient Factory observations. Astrophys J 788:17. doi:10.1088/0004-637X/788/1/17. arXiv:1405.1144

Chang C-K, Waszczak A, Lin H-W, Ip W-H, Prince TA, Kulkarni SR, Laher R, Surace J (2014b) A new large super-fast rotator: (335433) 2005 UW163. Astrophys J Lett 791:35. doi:10.1088/2041-8205/791/2/L35. arXiv:1407.8264

Chang C-K, Ip W-H, Lin H-W, Cheng Y-C, Ngeow C-C, Yang T-C, Waszczak A, Kulkarni SR, Levitan D, Sesar B, Laher R, Surace J, Prince TA (2015) Asteroid spin-rate study using the intermediate Palomar Transient Factory. Astrophys J Suppl Ser 27:219. doi:10.1088/0067-0049/219/2/27. arXiv:1506.08493

Chang C-K, Lin H-W, Ip W-H, Prince TA, Kulkarni SR, Levitan D, Laher R, Surace J (2016) Large super-fast rotator hunting using the intermediate Palomar Transient Factory. Astrophys J Suppl Ser 227:20. doi:10.3847/0067-0049/227/2/20. arXiv:1608.07910

Grav T, Mainzer AK, Bauer J, Masiero J, Spahr T, McMillan RS, Walker R, Cutri R, Wright E, Eisenhardt PRM, Blauvelt E, DeBaun E, Elsbury D, Gautier T IV, Gomillion S, Hand E, Wilkins A (2011) WISE/NEOWISE observations of the Jovian Trojans: preliminary results. Astrophys J 742:40. doi:10.1088/0004-637X/742/1/40. arXiv:1110.0280

Grillmair CJ, Laher R, Surace J, Mattingly S, Hacopians E, Jackson E, van Eyken J, McCollum B, Groom S, Mi W, Teplitz H (2010) An Overview of the Palomar

Chang *et al. Geosci. Lett.* (2017) 4:17

Page 8 of 8

Transient Factory Pipeline and Archive at the Infrared Processing and Analysis Center. In: Mizumoto Y, Morita K-I, Ohishi M (eds) Astronomical data analysis software and systems XIX, vol 434. Astronomical Society of the Pacific Conference Series, Waukesha, p 28

Harris AW, Young JW, Bowell E, Martin LJ, Millis RL, Poutanen M, Scaltriti F, Zappala V, Schober HJ, Debehogne H, Zeigler KW (1989) Photoelectric observations of asteroids 3, 24, 60, 261, and 863. Icarus 77:171–186. doi:10.1016/0019-1035(89)90015-8

Harris AW (1996) The rotation rates of very small asteroids: evidence for 'Rubble Pile' structure. In: Lunar and planetary science conference. Lunar and Planetary Inst. Technical Report, vol 27

Holsapple KA (2007) Spin limits of Solar System bodies: From the small fast-rotators to 2003 EL61. Icarus 187:500–509. doi:10.1016/j.icarus.2006.08.012

Jewitt D, Ishiguro M, Agarwal J (2013) Large particles in active asteroid P/2010 A2. Astrophys J Lett 764:5. doi:10.1088/2041-8205/764/1/L5. arXiv:1301.2566

Laher RR, Surace J, Grillmair CJ, Ofek EO, Levitan D, Sesar B, van Eyken JC, Law NM, Helou G, Hamam N, Masci FJ, Mattingly S, Jackson E, Hacopeans E, Mi W, Groom S, Teplitz H, Desai V, Hale D, Smith R, Walters R, Quimby R, Kasliwal M, Horesh A, Bellm E, Barlow T, Waszczak A, Prince TA, Kulkarni SR (2014) IPAC image processing and data archiving for the Palomar Transient Factory. Publ Astron Soc Pac 126:674–710. doi:10.1086/677351. arXiv:1404.1953

Law NM, Kulkarni SR, Dekany RG, Ofek EO, Quimby RM, Nugent PE, Surace J, Grillmair CC, Bloom JS, Kasliwal MM, Bildsten L, Brown T, Cenko SB, Ciardi D, Croner E, Djorgovski SG, van Eyken J, Filippenko AV, Fox DB, Gal-Yam A, Hale D, Hamam N, Helou G, Henning J, Howell DA, Jacobsen J, Laher R, Mattingly S, McKenna D, Pickles A, Poznanski D, Rahmer G, Rau A, Rosing W, Shara M, Smith R, Starr D, Sullivan M, Velur V, Walters R, Zolkower J (2009) The Palomar Transient Factory: system overview, performance, and first results. Publ Astron Soc Pac 121:1395–1408. doi:10.1086/648598. arXiv:0906.5350

Law NM, Dekany RG, Rahmer G, Hale D, Smith R, Quimby R, Ofek EO, Kasliwal M, Zolkower J, Velur V, Henning J, Bui K, McKenna D, Nugent P, Jacobsen J, Walters R, Bloom J, Surace J, Grillmair C, Laher R, Mattingly S, Kulkarni S (2010) The Palomar Transient Factory survey camera: first year performance and results. In: Ground-based and airborne instrumentation for astronomy III. Proceedings of the SPIE, vol 7735, p 77353. doi:10.1117/12.857400

Mainzer A, Grav T, Bauer J, Masiero J, McMillan RS, Cutri RM, Walker R, Wright E, Eisenhardt P, Tholen DJ, Spahr T, Jedicke R, Denneau L, DeBaun E, Elsbury D, Gautier T, Gomillion S, Hand E, Mo W, Watkins J, Wilkins A, Bryngelson GL, Del Pino Molina A, Desai S, Gómez Camus M, Hidalgo SL, Konstantopoulos I, Larsen JA, Maleszewski C, Malkan MA, Mauduit J-C, Mullan BL, Olszewski EW, Pforr J, Saro A, Scotti JV, Wasserman LH (2011) NEOWISE observations of near-Earth objects: preliminary results. Astrophys J 743:156. doi:10.1088/0004-637X/743/2/156. arXiv:1109.6400

Masiero JR, Mainzer AK, Grav T, Bauer JM, Cutri RM, Dailey J, Eisenhardt PRM, McMillan RS, Spahr TB, Skrutskie MF, Tholen D, Walker RG, Wright EL, DeBaun E, Elsbury D, Gautier T IV, Gomillion S, Wilkins A (2011) Main belt asteroids with WISE/NEOWISE. I. Preliminary albedos and diameters. Astrophys J 741:68. doi:10.1088/0004-637X/741/2/68. arXiv:1109.4096

Masiero J, Jedicke R, Ďurech J, Gwyn S, Denneau L, Larsen J (2009) The thousand asteroid light curve survey. Icarus 204:145–171. doi:10.1016/j.icarus.2009.06.012. arXiv:0906.3339

Mitchell JK, Houston WN, Carrier WD, Costes NC (1974) Apollo soil mechanics experiment S-200

Ofek EO, Laher R, Law N, Surace J, Levitan D, Sesar B, Horesh A, Poznanski D, van Eyken JC, Kulkarni SR, Nugent P, Zolkower J, Walters R, Sullivan M, Agüeros M, Bildsten L, Bloom J, Cenko SB, Gal-Yam A, Grillmair C, Helou G, Kasliwal MM, Quimby R (2012a) The Palomar Transient Factory photometric calibration. Publ Astron Soc Pac 124:62–73. doi:10.1086/664065. arXiv:1112.4851

Ofek EO, Laher R, Surace J, Levitan D, Sesar B, Horesh A, Law N, van Eyken JC, Kulkarni SR, Prince TA, Nugent P, Sullivan M, Yaron O, Pickles A, Agüeros M, Arcavi I, Bildsten L, Bloom J, Cenko SB, Gal-Yam A, Grillmair C, Helou G, Kasliwal MM, Poznanski D, Quimby R (2012b) The Palomar Transient Factory photometric catalog 1.0. Publ Astron Soc Pac 124:854–860. doi:10.1086/666978. arXiv:1206.1064

Polishook D, Ofek EO, Waszczak A, Kulkarni SR, Gal-Yam A, Aharonson O, Laher R, Surace J, Klein C, Bloom J, Brosch N, Prialnik D, Grillmair C, Cenko SB, Kasliwal M, Law N, Levitan D, Nugent P, Poznanski D, Quimby R (2012) Asteroid rotation periods from the Palomar Transient Factory survey. Mon Notices R Astron Soc 421:2094–2108. doi:10.1111/j.1365-2966.2012.20462.x. arXiv:1201.1930

Polishook D, Moskovitz N, Binzel RP, Burt B, DeMeo FE, Hinkle ML, Lockhart M, Mommert M, Person M, Thirouin A, Thomas CA, Trilling D, Willman M, Aharonson O (2016) A 2 km-size asteroid challenging the rubble-pile spin barrier—a case for cohesion. Icarus 267:243–254. doi:10.1016/j.icarus.2015.12.031. arXiv:1512.07088

Pravec P, Harris AW (2000) Fast and slow rotation of asteroids. Icarus 148:12–20. doi:10.1006/icar.2000.6482

Pravec P, Harris AW, Vokrouhlický D, Warner BD, Kušnirák P, Hornoch K, Pray DP, Higgins D, Oey J, Galád A, Gajdoš Š, Kornoš L, Világi J, Husárik M, Krugly YN, Shevchenko V, Chiorny V, Gaftonyuk N, Cooney WR, Gross J, Terrell D, Stephens RD, Dyvig R, Reddy V, Ries JG, Colas F, Lecacheux J, Durkee R, Masi G, Koff RA, Goncalves R (2008) Spin rate distribution of small asteroids. Icarus 197:497–504. doi:10.1016/j.icarus.2008.05.012

Pravec P, Kušnirák P, Šarounová L, Harris AW, Binzel RP, Rivkin AS (2002) Asteroids, comets, and meteors: ACM 2002. In: Warmbein B (ed) Large coherent asteroid 2001 OE84. ESA Special Publication, New York, pp 743–745

Rau A, Kulkarni SR, Law NM, Bloom JS, Ciardi D, Djorgovski GS, Fox DB, Gal-Yam A, Grillmair CC, Kasliwal MM, Nugent PE, Ofek EO, Quimby RM, Reach WT, Shara M, Bildsten L, Cenko SB, Drake AJ, Filippenko AV, Helfand DJ, Helou G, Howell DA, Poznanski D, Sullivan M (2009) Exploring the optical transient sky with the Palomar Transient Factory. Publ Astron Soc Pac 121:1334–1351. doi:10.1086/605911. arXiv:0906.5355

Rozitis B, Maclennan E, Emery JP (2014) Cohesive forces prevent the rotational breakup of rubble-pile asteroid (29075) 1950 DA. Nature 512:174–176. doi:10.1038/nature13632

Rubincam DP (2000) Radiative spin-up and spin-down of small asteroids. Icarus 148:2–11. doi:10.1006/icar.2000.6485

SDSS Collaboration (2000) The sloan digital sky survey: technical summary. Astron J 120:1579–1587. doi:10.1086/301513. arXiv:astro-ph/0006396

Salo H (1987) Numerical simulations of collisions between rotating particles. Icarus 70:37–51. doi:10.1016/0019-1035(87)90073-X

Tedesco EF, Cellino A, Zappalá V (2005) The statistical asteroid model. I. The main-belt population for diameters greater than 1 kilometer. Astron J 129:2869–2886. doi:10.1086/429734

Usui F, Kasuga T, Hasegawa S, Ishiguro M, Kuroda D, Müller TG, Ootsubo T, Matsuhara H (2013) Albedo properties of main belt asteroids based on the all-sky survey of the infrared astronomical satellite AKARI. Astrophys J 762:56. doi:10.1088/0004-637X/762/1/56. arXiv:1211.2889

Warner BD, Harris AW, Pravec P (2009) The asteroid lightcurve database. Icarus 202:134–146. doi:10.1016/j.icarus.2009.02.003

Waszczak A, Chang C-K, Ofek EO, Laher R, Masci F, Levitan D, Surace J, Cheng Y-C, Ip W-H, Kinoshita D, Helou G, Prince TA, Kulkarni S (2015) Asteroid light curves from the Palomar Transient Factory survey: rotation periods and phase functions from sparse photometry. Astron J 150:75. doi:10.1088/0004-6256/150/3/75. arXiv:1504.04041